

Surface-modified cobalt oxide nanoparticles: new opportunities for anti-cancer drug development

S. Chattopadhyay · S. P. Chakraborty · D. Laha ·
R. Baral · P. Pramanik · S. Roy

Received: 22 December 2011 / Accepted: 8 March 2012 / Published online: 27 May 2012
© Springer-Verlag 2012

Abstract The development of smart nanoparticles that can exhibit the anti-cancer activity, introduces better efficacy and lower toxicity for treatment. The present study was aimed to evaluate the anti-cancer activity of surface functionalized CoO nanoparticles against Jurkat (T-cell lymphoma) and KB (oral carcinoma) cell lines. The nano-sized cobalt oxide nanoparticles (CoO) was prepared by thermal decomposition method followed by surface modification using phosphonomethyl iminodiacetic acid (PMIDA). The PMIDA-coated CoO nanoparticle was characterized by X-ray diffraction, dynamic light scattering, and transmission electron microscopy; and the conjugation was analyzed by Fourier transform infrared spectroscopy. The resultant nanoparticles with an average size less than 100 nm measured by dynamic light scattering and transmission electron microscopy. Cytotoxicity study, flow cytometric analysis and scanning electron micrographs have been revealed that PMIDA-coated nanoparticles significantly enhances the cellular uptake of the nanoparticle and thus facilitates apoptosis of cancer cell (Jurkat and KB). For the application of PMIDA-coated CoO nanoparticles in the

medical field, doxorubicin, a potent anti-cancer drug, has been used in similar fashion in this experimental design and all these effects or patterns were observed.

Keywords Cobalt oxide nanoparticles · Cancer cell line · Anti-cancer drug · Cytotoxicity · Cellular apoptosis · SEM micrographs

1 Introduction

The rapid developments of various modified nanoparticles (NP) are attracting increased attention because of their potential in a wide range of biotechnological applications, especially in advance biomedical application (Liong et al. 2008), drug delivery systems (Cheng et al. 2006), and vaccine administration (Schreiber et al. 2010). One of the most interesting chemical elements used as nanoparticles for biomedical applications is cobalt (Co) which is mainly used as cobalt oxide and has an organo-metal compound or a biopolymer (Wang et al. 2005). In spite of its physiological role as a co-factor of vitamin B₁₂, cobalt cannot be regarded only as an essential element. Cobalt-based NPs, in general, cobalt oxide nanoparticles, in particular, are currently attracting enormous interest owing to their unique size- and shape-dependent properties and potential applications in pigments, catalysis, sensors, electrochemistry, magnetism, energy storage, etc. (Liu et al. 2005).

The uses of polymeric nanoparticles with functional properties have been widely used in a broad range of bio applications; like drug and gene delivery, cell and tissue engineering, diagnostic and therapeutic purposes etc. (Uhrich et al. 1999; Panyam and Labhasetwar 2003; Marin et al. 2005; Marinakos et al. 2001). Among these applications, the field of drug delivery by nanoparticles with

S. Chattopadhyay · S. P. Chakraborty · S. Roy (✉)
Immunology and Microbiology Laboratory, Department of Human
Physiology with Community Health, Vidyasagar University,
Midnapore 721 102 West Bengal, India
e-mail: roysomenath@hotmail.com

D. Laha · P. Pramanik
Nano materials Laboratory, Department of Chemistry,
Indian Institute of Technology,
Kharagpur, West Bengal, India

R. Baral
Immunoregulation and Immunodiagnosics,
Chittaranjan National Cancer Institute,
Kolkata 700 026, India

specific and rapid internalization into a target cell has immense promise (Maeda et al. 2009; Faraji and Wipf 2009; Singh and Lillard 2009; Breunig et al. 2008; Brannon-Peppas and Blanchester 2004). Nanoparticles of polymer not only protect the bioactive substance but also facilitate the control release of the material in delivering system (Vauthier et al. 2003; Liang et al. 2006; Sheikh et al. 2009; Mitra et al. 2001). Therefore, in the present paper, we have focused our interest on the study of modified CoO NPs. Believing that the characterization of the physical–chemical properties of NP is relevant for the study of their biological activity, we analyzed CoO NP morphology by electron microscopy in order to define aggregation, size, and shape. These properties may have a significant influence on their biological effects. This present study was aimed to develop a novel and economically viable nanoparticles which have anti-cancer activity to cancer cell in vitro.

2 Materials and methods

2.1 Chemicals and reagents

Phosphonomethyl iminodiacetic acid (PMIDA), propidium iodide, cobalt chloride ($\text{CoCl}_2 \cdot 3\text{H}_2\text{O}$), RNaseA, 3-(4,5-dimethyl-2-thiazolyl)-2,5-diphenyl-2H-tetrazolium bromide (MTT reagent), Histopaque 1077, and Rhodamine isothiocyanate (RITC) were procured from Sigma (St. Louis, MO, USA). Minimum essential medium (MEM), RPMI 1640, fetal bovine serum (FBS), penicillin, streptomycin, doxorubicin, sodium chloride (NaCl), sodium carbonate (Na_2CO_3), sucrose, Hanks balanced salt solution, and ethylene diamine tetra acetate were purchased from Himedia, India. Tris–HCl, Tris buffer, KH_2PO_4 , K_2HPO_4 , HCl, formaldehyde, alcohol, and other chemicals were procured from Merck Ltd., SRL Pvt. Ltd., Mumbai, India. Commercially available dimethyl sulfoxide was procured from Himedia, India, and was purified by vacuum distillation over KOH. All other chemicals were from Merck Ltd., SRL Pvt., Ltd., Mumbai, and were of the highest purity grade available.

2.2 Synthesis of cobalt oxide nanoparticles

Cobalt oxide NPs were prepared by thermal decomposition method. The starting materials were $\text{CoCl}_2 \cdot 3\text{H}_2\text{O}$, Na_2CO_3 . Two grams of starting material ($\text{CoCl}_2 \cdot 3\text{H}_2\text{O}$) was taken in a beaker and mixed with Na_2CO_3 as a molar ratio 1:1. Then the solution was rotated 1 h at room temperature. After that the precipitations were collected by centrifugation to obtain the nanoparticle precursor. The precursor was calcinated at 300 °C in air in a porcelain crucible for 2 h to get cobalt oxide NPs.

2.3 Surface modification of synthesized cobalt oxide nanoparticles

Thirty milligrams of synthesized cobalt oxide NPs was dispersed in 10 ml of milli-Q (Millipore) to make a solution 3 mg/ml. Another solution of PMIDA was prepared by dissolving 27 mg PMIDA in 10 ml of distilled water. Then this solution was mixed with above solution. The pH of the medium was maintained at 10 and stirring for 12 h. After that particles were collected by centrifugation. Then the recovered particles were washed three times with milli-Q (Millipore).

2.4 Characterization of synthesized surface modified cobalt nanoparticles

2.4.1 X-ray diffraction study

The phase formation and crystallographic state of cobalt oxide NPs were determined by XRD with an Expert Pro (Phillips) X-ray diffractometer using $\text{CoK}\alpha$ radiation ($\lambda=0.178$ nm). Samples were scanned from 20° to 80° of 2θ increment of 0.04° with 2 s counting time. Hydrodynamic size of the cobalt oxide nanoparticles aggregates was measured in a Brookhaven 90 Plus particle size analyzer (Chakraborty et al. 2010).

2.4.2 Dynamic light scattering

Dynamic light scattering (DLS) analysis was done by Zetasizer Nano ZS (Malvern Instruments) according to the method of Chakraborty et al. (2010) with some modifications. The concentration of the cobalt oxide nanoparticles was 100 $\mu\text{g}/\text{ml}$ and was sonicated for 2 min and dynamic particle sizes were measured suspending two drops of aqueous suspension of nanoparticles in 10 ml of Millipore water. When particle was completely dispersed in water then particle was analyzed with a dynamic light scattering analyzer. The experiments were repeated several times to get average size of nanoparticles.

2.4.3 Transmission electron microscopy

The particle size and microstructure were studied by high-resolution transmission electron microscopy in a JEOL 3010, Japan operating at 200 kV according to the method of Chakraborty et al. (2010) with some modifications. In brief, cobalt oxide nanoparticles was suspended in deionized at a concentration of 1 mg/ml then the sample was sonicate using a sonicator bath until sample form a homogenous suspension. For size measurement, sonicated stock solution of all cobalt oxide nanoparticles (0.5 mg/ml) was diluted 20 times. TEM was used to characterize the size and shape of the cobalt oxide nanoparticles. A drop of aqueous cobalt oxide nanoparticles suspension was placed on to carbon-coated copper grid and this was dried in air to get TEM image.

2.4.4 Fourier transform infrared spectroscopy

The conjugation of PMIDA with CoO nanoparticles was investigated by the FTIR with a model Thermo Nicolet Nexux-model 870 according to the method of Chakraborty et al. (2010) with some modifications. In brief, 1.0 mg sticky mass of PMIDA-coated CoO nanoparticles with 100 μ l KBr medium and a thin film was prepared on the NaCl plate by drop casting method and under atmosphere separately. The FTIR value was taken within 500 to 4,000 wave numbers (cm^{-1}).

2.5 Selection of human subjects for collection of lymphocytes and oral squamous epithelial cell

Six healthy subjects were chosen to collect the blood sample for separation of lymphocytes and collection of squamous epithelial cell by scraping. All subjects enrolled in this study were asymptomatic and none of them had abnormality on physical examinations and routine laboratory tests. All the subjects were from same geographical area and same economic status, non-smokers and non-alcoholic, and having same food habit. These subjects received no medication, including vitamin E and vitamin C. All subjects gave informed consent. The selection excluded not only individuals with acute infections or chronic diseases, but also excluded healthy individuals undergoing supplementation with antioxidative substances. The study protocol was in accordance with the declaration of Helsinki, and was approved by the ethical committee of Vidyasagar University.

2.5.1 Separation of lymphocytes

Fasting blood samples were collected from all groups of individuals satisfying the Helsinki protocol. The lymphocytes were isolated from heparinized blood samples according to the method of Hudson and Hay (Hudson et al. 1991). Blood was taken and diluted with phosphate-buffered saline (pH 7.0) in equal ratio and then layered very carefully on the density gradient (histopaque) in 1:2 ratio, centrifuged at $500\times g$ for 40 min and the white milky layer of mononuclear cells, i.e., lymphocytes were carefully removed. The layer was washed twice with the same buffer and then centrifuged at 2400 rpm for 10 min to get the required pellet of lymphocytes.

2.5.2 Collection of oral squamous epithelial cells

Mucosal scrapings were placed in medium MEM supplemented with 10 % fetal bovine serum and then passed through a sterile 100-mm nylon mesh followed by further washes with MEM complete medium. Filtrate was

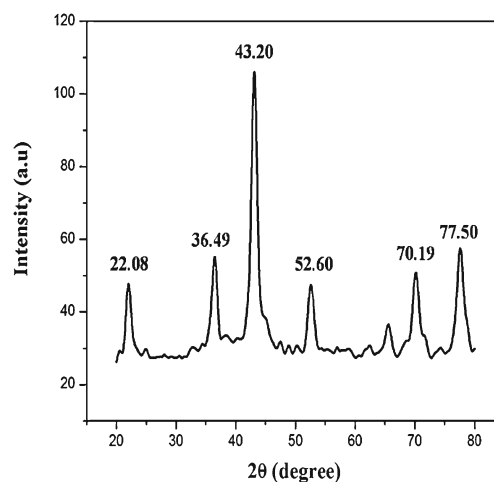


Fig. 1 X-ray diffraction analysis of cobalt oxide nanoparticles

then centrifuged at 2,200–2,400 rpm for 5 min and the supernatant discarded. The cell pellet is suspended in MEM supplemented with 10 % fetal bovine serum, 100 μ g/ml streptomycin, and 100 U/ml penicillin (Steele and Fidel 2002).

2.6 Cell culture

The normal human lymphocytes and oral squamous epithelial cells, T-cell lymphoma (Jurkat) and oral epithelial cancer (KB) cell lines were cultivated for in vitro experiments. Cell lines were obtained from the National Centre for Cell Sciences, Pune, India. It was cultured in RPMI 1640 medium and minimal essential medium supplemented with 10 % fetal calf serum, 100 U/ml penicillin, and 100 μ g/ml streptomycin, 4 mM L-glutamine under 5 % CO_2 , and 95 % humidified atmosphere at 37 $^\circ\text{C}$.

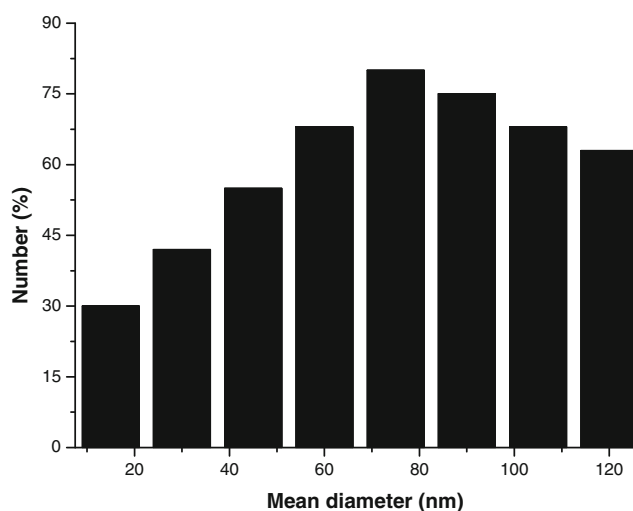


Fig. 2 The size determination of cobalt oxide nanoparticles by dynamic light scattering

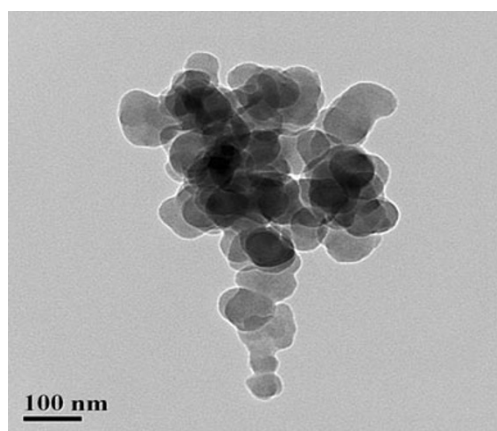


Fig. 3 TEM images of PMIDA-coated cobalt oxide nanoparticles

2.7 Preparation of drug

Several doses of PMIDA-coated CoO nanoparticles and doxorubicin (1–25 $\mu\text{g/ml}$) were prepared using sterile phosphate buffer saline (pH 7.4). In this study, all these doses were charged against normal and cancer cell line for evaluation of *in vitro* anti-cancer activity.

2.8 Experimental design

Each type of cells was divided into nine groups. Each group contained six Petri dishes (2×10^5 cells in each). The cells of each Petri dishes of control and experimental groups were maintained in MEM and RPMI 1640 media, where as it is applicable, supplemented with 10 % FBS, 50 $\mu\text{g/ml}$ gentamycin, 50 $\mu\text{g/ml}$ penicillin, and 50 $\mu\text{g/ml}$ streptomycin at

37 °C in a 95 % air/5 % CO_2 atmosphere in CO_2 incubator. The following groups were considered for the experiment and cultured for 48 h:

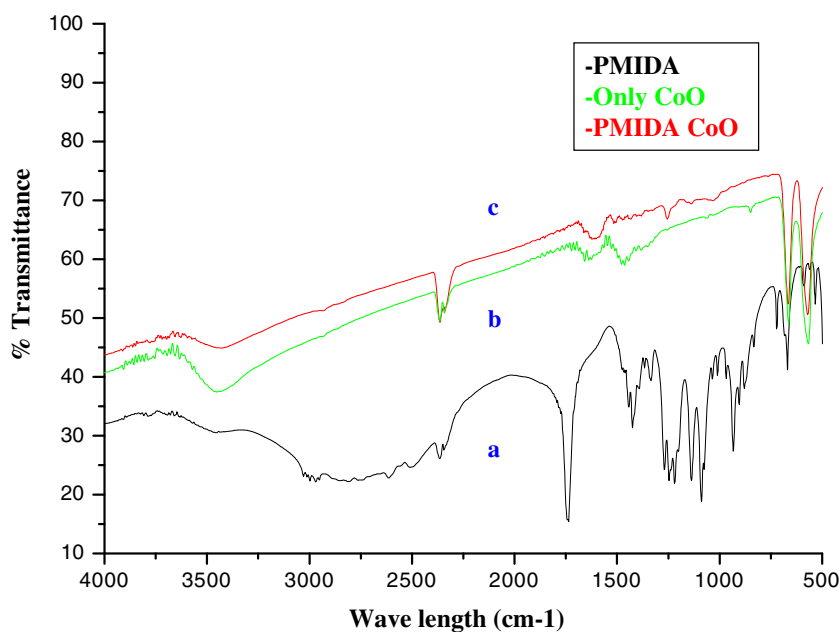
- Group I Control, i.e., cells in culture media
- Group II Cells+1 $\mu\text{g/ml}$ doxorubicin in culture media
- Group III Cells+1 $\mu\text{g/ml}$ PMIDA-coated CoO nanoparticles in culture media
- Group IV Cells+5 $\mu\text{g/ml}$ doxorubicin in culture media
- Group V Cells+5 $\mu\text{g/ml}$ PMIDA-coated CoO nanoparticles in culture media
- Group VI Cells+10 $\mu\text{g/ml}$ doxorubicin in culture media
- Group VII Cells+10 $\mu\text{g/ml}$ PMIDA-coated CoO nanoparticles in culture media
- Group VIII Cells+25 $\mu\text{g/ml}$ doxorubicin in culture media
- Group IX Cells+25 $\mu\text{g/ml}$ PMIDA-coated CoO nanoparticles in culture media

After the treatment schedule, the cells were collected from the Petri dishes separately and centrifuged at 2,200 rpm for 10 min at 4 °C. The cells were washed twice with 50 mM PBS, pH 7.4 and then processed for the biochemical estimation (Sandhu and Kaur 2002).

2.9 *In vitro* cytotoxicity

Normal human lymphocytes and oral squamous epithelial cell, Jurkat and KB cell lines were seeded into 96 wells of tissue culture plates having 180 μl of complete media and were incubated for 48 h. Doxorubicin and PMIDA-coated CoO nanoparticles were added to the cells at different concentrations (1, 5, 10, and 25 $\mu\text{g/ml}$), were incubated for 48 h at 37 °C in a humidified incubator (NBS) maintained with 5 % CO_2 . The

Fig. 4 FTIR spectra of *a* PMIDA, *b* cobalt oxide nanoparticles, and *c* PMIDA-coated cobalt oxide nanoparticles



cell viability was estimated by 3-(4,5-dimethylthiazol)-2-diphenyltetrazolium bromide according to the method of our previous laboratory report Chakraborty et al. 2011.

2.10 Detection of cellular apoptosis by flow cytometric analysis using propidium iodide

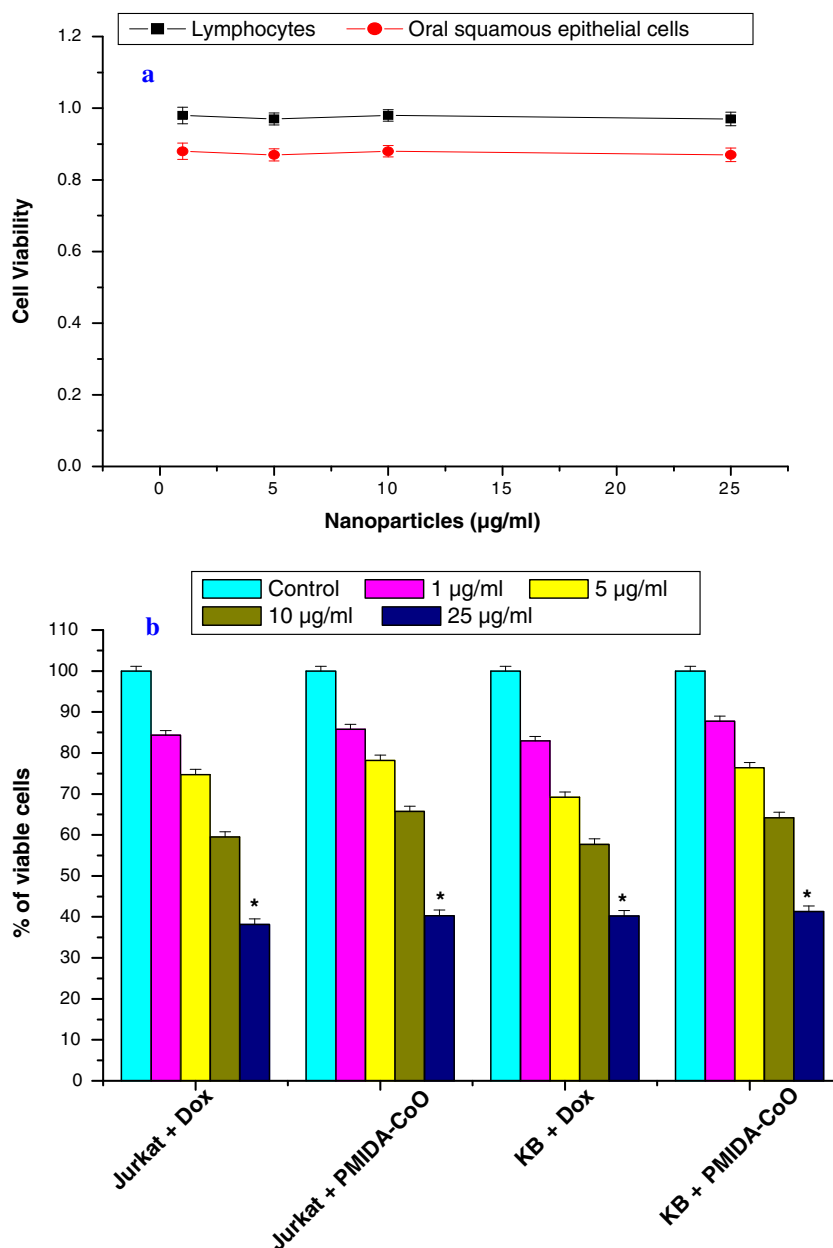
Cell apoptosis was measured using propidium iodide staining and analysis by flow cytometry (Roa et al. 2009). After the treatment schedule; the cells were scraped and centrifuged with the supernatant medium at 3,500 rpm for 5 min. Following washes, cells were resuspended in PBS and fixed in 70 % ethanol for 1 h on ice. Fixed cells were washed with

PBS and stained with propidium iodide (5 µg/mL) solution containing ribonuclease (RNase; 50 µmol/L) for 30 min at room temperature. Then, cells were analyzed on a Becton Dickinson FACS Calibur flow cytometer. The sub-G0 population of the cells was determined by CellQuest software.

2.11 Alteration of cellular morphology by scanning electron microscope

After the treatment schedule, Jurkat and KB cells were examined under electron microscope according to the method of Papis et al. (2009) to visualize whether the cell undergoes for morphological alteration or not. In brief, treated cells were

Fig. 5 Cytotoxicity of PMIDA-coated cobalt oxide nanoparticles against normal human lymphocytes and squamous epithelial cell (a) and human T-cell lymphoma and oral squamous carcinoma cell lines (b). *n*=6; values are expressed as mean±SEM. Asterisks indicate the significant difference as compared to control group



harvested, fixed in 2 % glutaraldehyde in 0.1 M Na-cacodylate buffer (pH 7.2) for 1 h at room temperature, washed in the same buffer, and post fixed for 1 h with 1 % osmium tetroxide in 0.1 M Na-cacodylate buffer (pH 7.2) at room temperature and dehydrated in graded ethanol and observed under electron microscope.

2.12 Intracellular uptake

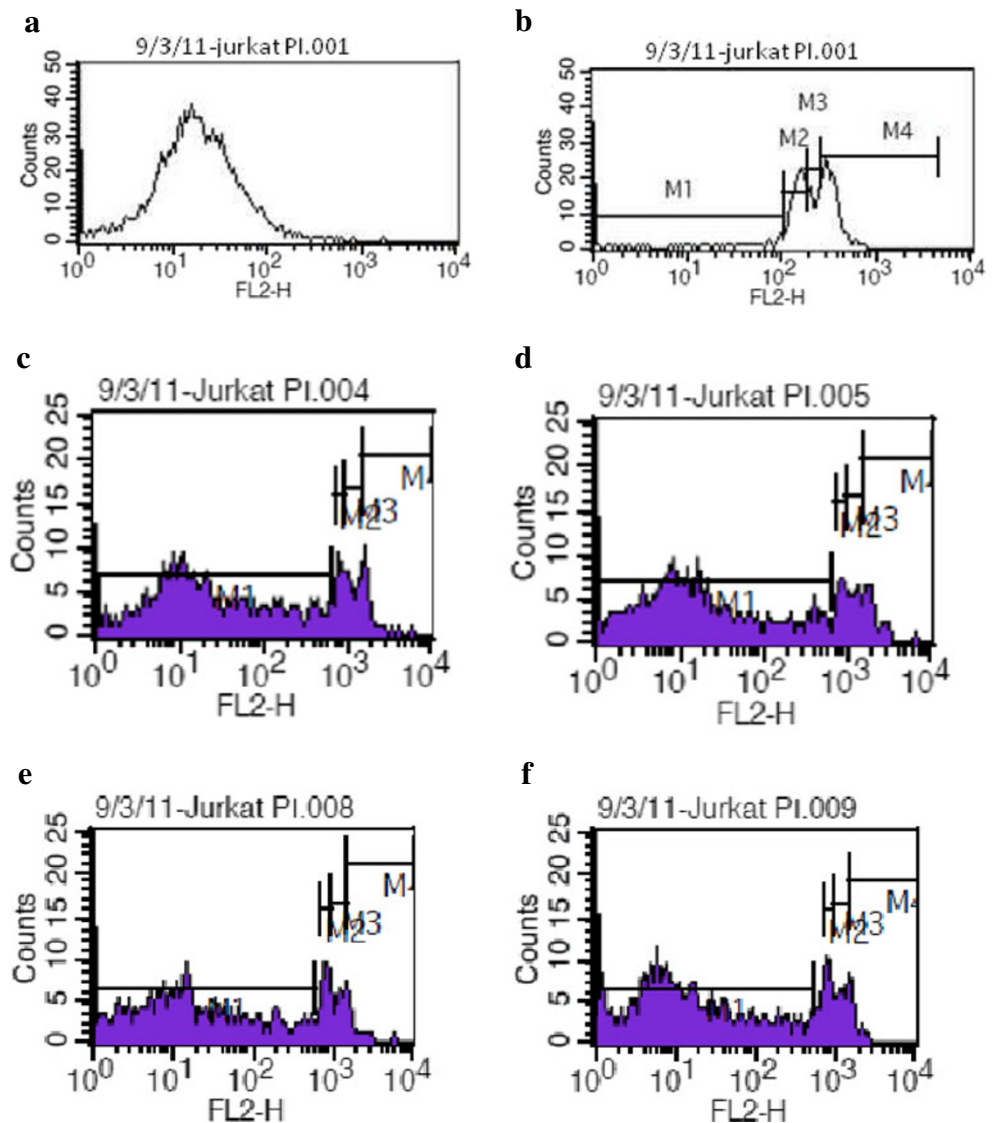
Nanoparticle uptake by Jurkat and KB cells was studied by fluorescence microscopy methods according to our previous laboratory report (Sahu et al. 2010). After the treatment schedule, 2×10^5 cells were seeded into 35 mm cell culture plates. It was incubated in a humidified incubator maintained with 5 % CO₂ and 37 °C. After 8 h the cells were washed with incomplete media and were incubated with 25 µg/ml DOX/DOX-RITC and PMIDA-coated CoO NP/PMIDA-coated CoO NP-RITC

for fluorescence microscopy. Then the cells were allowed to adhere to a glass cover slip in 35-mm Petriplates, followed by incubation for 4 h at 37 °C in a humidified incubator maintained with 5 % CO₂. Fluorescence images were acquired with 488 nm laser for differential interference contrast microscopy and 543 nm lasers for RITC excitation on an Olympus research phase contrast with fluorescence microscope (model: CX41; Olympus Singapore Pvt. Ltd., Valley Point Office Tower, Singapore).

2.13 Statistical analysis

The data were expressed as mean±SEM, $n=6$. Comparisons between the means of control and treated group were made by one-way ANOVA test (using a statistical package, Origin 6.1, Northampton, MA 01060 USA) with multiple comparison *t* tests, $p < 0.05$ as a limit of significance.

Fig. 6 PMIDA-coated cobalt oxide nanoparticles induced cellular apoptosis analysis in Jurkat cell lines by flow cytometry using propidium iodide. Here **a** -ve control, **b** +ve control, **c** Jurkat+10 µg/ml PMIDA-coated CoO nanoparticles, **d** Jurkat+10 µg/ml doxorubicin, **e** Jurkat+25 µg/ml PMIDA-coated CoO nanoparticles, **f** Jurkat+25 µg/ml doxorubicin



3 Result and discussion

3.1 Synthesis of PMIDA-coated CoO nanoparticles

Several data are available about the toxicology of cobalt ions, it is generally accepted that the biological activity and potential toxicity of metallic NPs cannot simply be derived from previous data on ionic forms, indicating the importance of testing the effects of chemicals in nanostructural form (Roco 2005). The nano-sized cobalt oxide nanoparticles (CoO) was prepared by thermal decomposition method followed by surface modification using phosphonomethyl iminodiacetic acid. The phosphonate group of the *N* phosphonomethyl iminodiacetic acid ligand acts as a surface anchoring

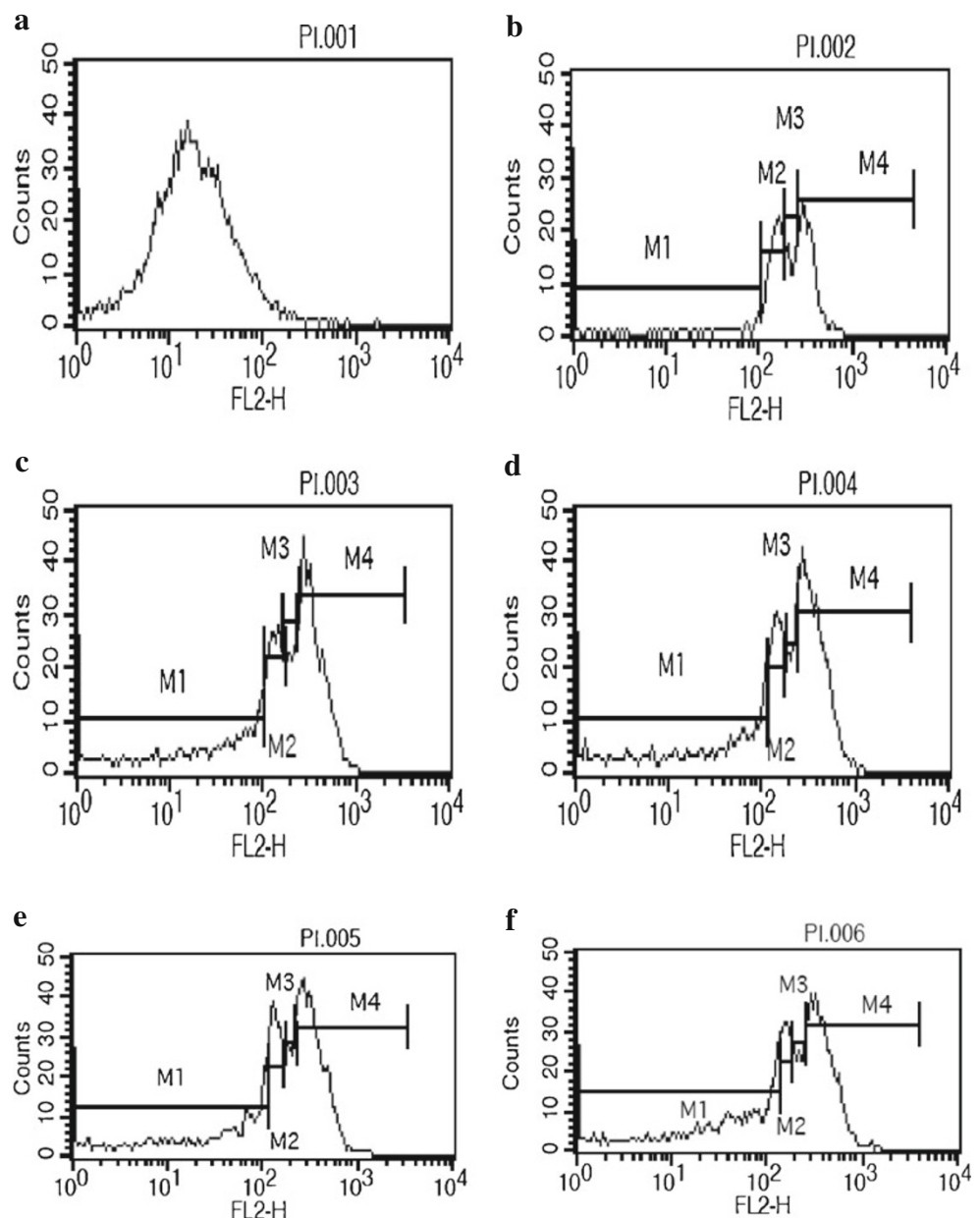
agent on nanoparticles and the $-COOH$ remains free at outside.

3.2 Characterization of synthesized surface modified cobalt nanoparticle

3.2.1 X-ray diffraction analysis

The XRD pattern of cobalt oxide nanoparticle were compared and interpreted with standard data of JCPDS file (JCPDS international center for diffraction data, 1991). The XRD pattern of cobalt oxide nanoparticles was represented in Fig. 1. The characteristic peaks at $2\theta=22.08^\circ$, 36.49° , 43.20° , 52.60° , 70.19° , and 77.500 for cobalt oxide nanoparticles,

Fig. 7 PMIDA-coated cobalt oxide nanoparticles induced cellular apoptosis analysis in KB cell lines by flow cytometry using propidium iodide. Here **a** -ve control, **b** +ve control, **c** KB+10 $\mu\text{g/ml}$ PMIDA-coated CoO nanoparticles, **d** KB+10 $\mu\text{g/ml}$ doxorubicin, **e** KB+25 $\mu\text{g/ml}$ PMIDA-coated CoO nanoparticles, **f** KB+25 $\mu\text{g/ml}$ doxorubicin



which are marked respectively by their indices (111), (220), (311), (400), (511), and (440) agreement with JCPDS card no 73-1701. The X-ray pattern confirmed the phase formation of cobalt oxide nanoparticle.

3.2.2 Dynamic light scattering experiment

The size distribution of cobalt oxide nanoparticles in aqueous medium was characterized by DLS. The mean size of nanoparticles in aqueous solution was determined to be 70 ± 12 nm shown in Fig. 2. This study of the particle was further confirmed by the presence of stable, non aggregate of cobalt oxide nanoparticle.

3.2.3 Transmission electron microscopy

The TEM morphology of cobalt oxide nanoparticles shows having nearly spherical geometry with a mean size of less

than 100 nm. The result was represented in Fig. 3. The presence of some bigger particle should be attributed to be aggregating or overlapping of some small particle. The observed nanoparticles size was approximately larger than the hydrodynamic diameter obtained from the DLS experiment. In TEM described the size in the dried state of the sample, whereas DLS measured the size in the hydrated state of the sample, so that the size measured by DLS was a hydrodynamic diameter and had a larger. However, one has to bear in mind that by TEM we image single particles, while DLS gives an average size estimation, which is biased toward the larger-size end of the population distribution.

3.2.4 Fourier transform infrared spectroscopy

Conjugation of PMIDA with CoO nanoparticles was investigated by FTIR spectroscopy. The comparison of FTIR spectrum of pure CoO nanoparticles, PMIDA, and PMIDA-coated

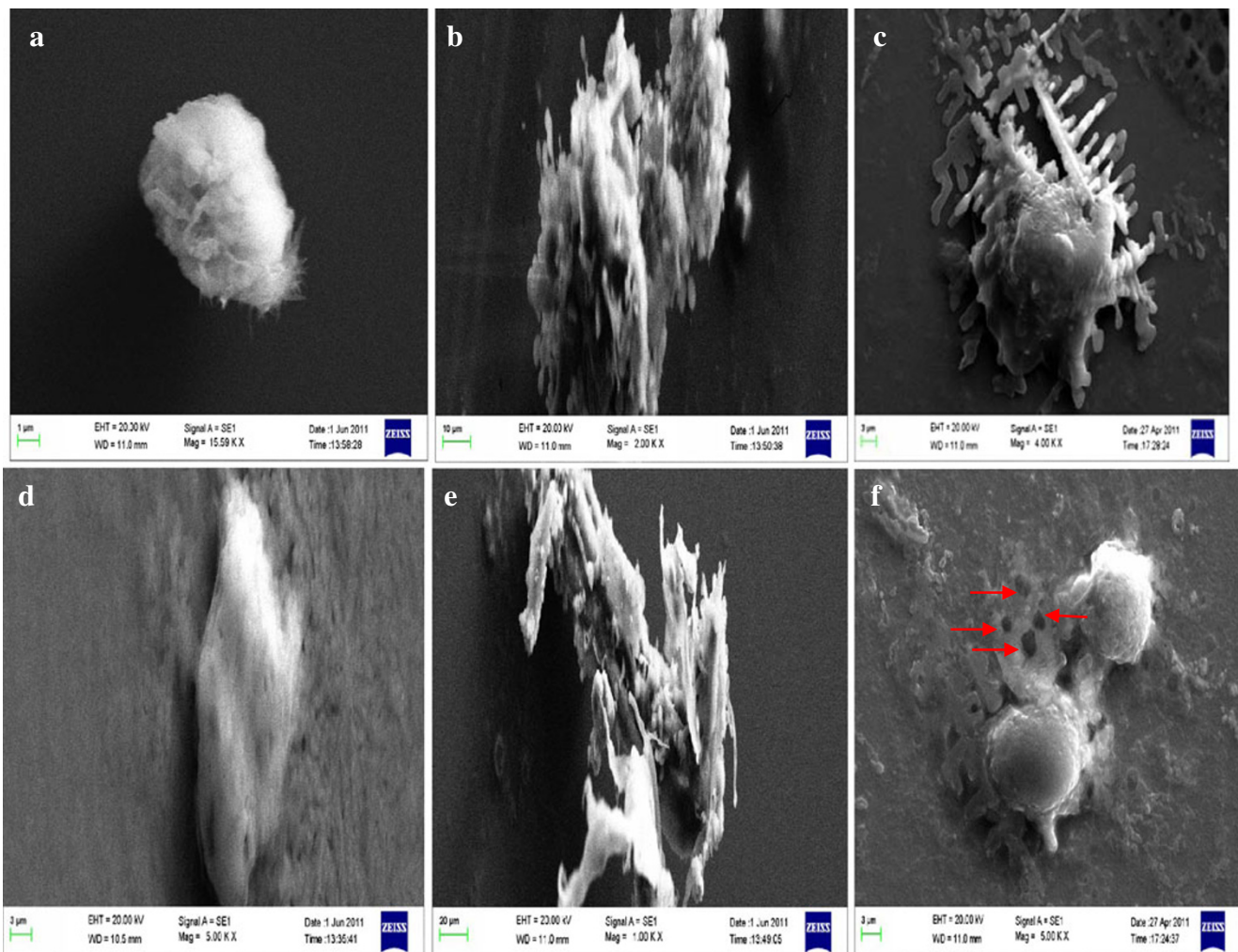


Fig. 8 Scanning electron microscopy shows the intracellular uptake of PMIDA-coated cobalt oxide nanoparticles into Jurkat and KB cell lines. **a** Jurkat control, **b** Jurkat+25 $\mu\text{g/ml}$ doxorubicin, **c** Jurkat+

25 $\mu\text{g/ml}$ PMIDA-coated CoO nanoparticles, **d** KB control, **e** KB+25 $\mu\text{g/ml}$ doxorubicin, **f** KB+25 $\mu\text{g/ml}$ PMIDA-coated CoO nanoparticles

CoO are shown in Fig. 4. FTIR spectra shows basic characteristics IR band of CoO at 570 cm^{-1} , which indicate presence of CoO vibration and a broad band around $3,440\text{ cm}^{-1}$ indicative the presence of $-\text{OH}$ groups on the nanoparticle surface. After conjugation of PMIDA on nanoparticle surface a significant decrease in the intensity of the band at $3,440\text{ cm}^{-1}$ which indicates the conjugation of phosphonic acid on CoO NPs. A significant band also show at $1,050\text{ cm}^{-1}$, $1,750\text{ cm}^{-1}$ for $\text{M}-\text{O}-\text{P}$ and $\text{P}=\text{O}$ respectively which also confirm the successful conjugation of PMIDA on nanoparticle surface.

3.3 In vitro toxicity studies

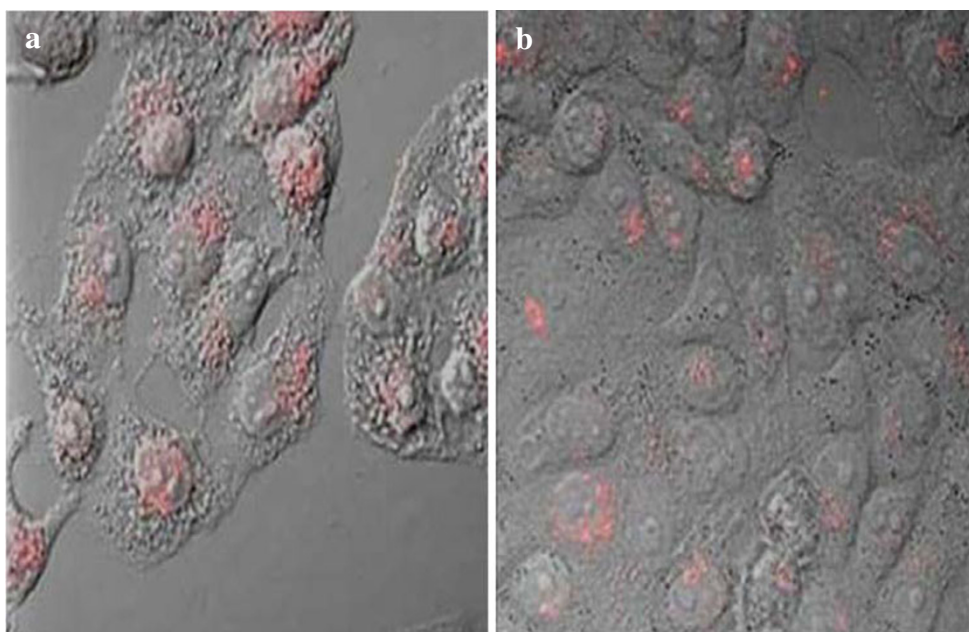
The toxicity of the PMIDA-coated CoO nanoparticles was checked towards normal human lymphocytes and oral squamous epithelial cell in vitro. PMIDA-coated CoO nanoparticles mediated cytotoxicity to these normal cells was measured by MTT assay (Fig. 5). It was found that there was no significant difference in cell viability between the cells treated with PMIDA-coated CoO nanoparticles and the cell treated without PMIDA-coated CoO nanoparticles. It was represented in Fig. 5a. Hence these nanoparticles are expected to be safe for biomedical application. On the other hand, surprisingly PMIDA-coated CoO nanoparticles exhibits anti-cancer activity against Jurkat and KB cell lines in a dose-dependent fashion. It was observed from our experiment, doxorubicin kills the Jurkat cell and KB cell by 15.64 %, 25.28 %, 40.52 % and 17.08 %, 30.80 %, 42.73 %, respectively, at a dose of 1, 5, and 10 $\mu\text{g}/\text{ml}$; whereas PMIDA-coated CoO nanoparticles kills the Jurkat and KB cells by 14.2 %, 21.80 %, 34.28 % and 12.20 %, 23.58 %, 35.78 %, respectively. All these changes were insignificant at the level of $p < 0.05$ (Fig. 5b). But 25 $\mu\text{g}/\text{ml}$ doxorubicin and PMIDA-

coated CoO nanoparticles kills the Jurkat and KB cells significantly ($p < 0.05$) by 61.85 %, 59.76 % and 58.71 %, 59.71 %, respectively (Fig. 5b). So, it was observed from our results that PMIDA-coated CoO nanoparticles has little bit least effect on Jurkat and KB cell lines than doxorubicin treatment. But our previous experimental data (Fig. 5a) showed that PMIDA-coated CoO nanoparticles have no toxic effect on normal human lymphocytes and oral squamous epithelial cells. Previous research by Karim and his colleagues in 2001 and Dhawan and his colleagues in 2003 reported that doxorubicin has toxic effect on normal cells. In this point of view, PMIDA-coated CoO nanoparticles may have a great promise in the treatment of cancer because of its no lethal toxicity on normal cells.

3.4 Cellular apoptosis analysis by flow cytometry using propidium iodide

To investigate whether PMIDA-coated CoO nanoparticles is associated with the induction of cellular apoptosis, after the treatment schedule Jurkat and KB cells were analyzed fluorescence-activated cell sorter with propidium iodide. PMIDA-coated CoO nanoparticles induced the cellular apoptosis in Jurkat cell lines by 63.25 % and 65.93 %; where as 37.39 % and 38.77 % in KB cell line. In contrast, doxorubicin shows 77.53 % and 78.05 % cellular apoptosis in Jurkat cell lines; whereas and 37.20 % and 46.64 % in KB cell lines of 10 and 25 $\mu\text{g}/\text{ml}$ of PMIDA-coated CoO nanoparticles (Figs. 6 and 7). The cell cycle pattern of those two cancer cell line shows that the cellular apoptosis proceed because the nanoparticles has the ability to alter the intracellular antioxidant regulation and plasma membrane structure which leads the cell to undergo apoptosis.

Fig. 9 Fluorescence micrograph shows the intracellular uptake of PMIDA-coated cobalt oxide nanoparticles into Jurkat (a) and KB (b) cell lines



3.5 Intracellular uptake by scanning electron microscopy and fluorescence imaging

Nanoparticles binding to the plasma membrane and cellular uptake are probably a necessary condition for its exertion of cytotoxicity. We have shown that PMIDA-coated CoO nanoparticles were taken up by Jurkat and KB cell lines in *in vitro* cultures and the alteration of cellular structure was observed (Fig. 8). From the fluorescence images (Fig. 9) the PMIDA-coated CoO nanoparticles were found to be distributed in the cytoplasm leaving clear zone of nucleus, indicating cellular uptake instead of adhesion to the surface and the nanoparticles preferentially targeted the cancer cells and were internalized. This internalization might be due to the receptor-mediated endocytosis (Peters et al. 2007; Gojova et al. 2007; Mohapatra et al. 2007).

4 Conclusion

In this study, a simple process has been developed to synthesize PMIDA-coated CoO nanoparticles. This nano polymeric system impact excellent stability in aqueous medium with reasonable good hydrodynamic size. *In vitro* cytotoxicity test using an MTT assay method showed that this PMIDA-coated CoO nanoparticles has anti-cancer activity; rather than they have no adverse effect on normal cells. Flow cytometry has revealed that nanoparticles are targeting more effectively the cancerous cells. Due to high specific uptake, this system may further be explored for the application of new anti-cancer drug development therapy. The data presented here suggests that further *in vivo* studies are needed to define the therapeutic index of the tumor-targeting polymeric carrier and will constitute the basis for the next generation drug development. *In vivo* testing of anti-cancer activity of these nanoparticles is in progress.

Acknowledgment The authors express gratefulness to the Department of Biotechnology, Government of India, for funding. The authors also express gratefulness to the Indian Institute of Technology, Kharagpur and Vidyasagar University, Midnapore, for providing the facilities to execute these studies.

Declaration of interest Authors declare that there are no conflicts of interests.

References

- Brannon-Peppas L, Blanchester JO (2004) Nanoparticles and targeted system for cancer therapy. *Adv Drug Deliv Rev* 56:1649–1659. doi:10.1016/j.addr.2004.02.014
- Breunig M, Bauer S, Goepferich A (2008) Polymers and nanoparticles: intelligent tools for intracellular targeting. *Eur J Pharm Biopharm* 68:112–128. doi:10.1016/j.ejpb.2007.06.010
- Chakraborty SP, Sahu SK, Kar Mahapatra S, Santra S, Bal M, Roy S, Pramanik P (2010) Nanoconjugate vancomycin: new opportunities for the development of anti-VRSA agents. *Nanotechnology* 21:105103. doi:10.1088/0957-4484/21/10/105103
- Chakraborty SP, Sahu SK, Pramanik P, Roy S (2011) Biocompatibility of folate-modified chitosan nanoparticles. *Asian Pacific J of Tropical Biomedicine* 2(3):215–219
- Cheng J, Teply BA, Jeong SY, Yim CH, Ho D, Sherif I, Jon S, Farokhzad OC, Khademhosseini A, Langer RS (2006) Magnetically responsive polymeric microparticles for oral delivery of protein drugs. *Pharm Res* 23:557–564. doi:10.1007/s11095-005-9444-5
- Dhawan A, Kayani MA, Parry JM, Parry E, Anderson D (2003) Aneugenic and clastogenic effects of doxorubicin in human lymphocytes. *Mutagenesis* 18(6):487–490. doi:10.1093/mutage/geg024
- Faraji AH, Wipf P (2009) Nanoparticles in cellular drug delivery. *Bioorg Med Chem* 17:2950–2962. doi:10.1016/j.bmc.2009.02.043
- Gojova A, Guo B, Kota RS, Rutledge JC, Kennedy IM, Barakat AI (2007) Induction of inflammation in vascular endothelial cells by metal oxide nanoparticles: effects of particle composition. *Environ Health Persp* 115:403–409. doi:10.1289/ehp.8497
- Hudson L, Hay FC (1991) *Practical immunology*, 3rd Ed. Blackwell Scientific Publications, Oxford. 21–22
- Karim S, Bhandari U, Kumar H, Salam A, Siddiqui M, Pillai KK (2001) Doxorubicin-induced cardiotoxicity and its modulation by drugs. *Ind J Pharmacol* 3:203–207
- Liang HF, Chen CT, Chen SC, Kulkarni AR, Chiu YL, Chen MC et al (2006) Paclitaxel-loaded poly(g-glutamic acid)-poly(lactide) nanoparticles as a targeted drug delivery system for the treatment of liver cancer. *Biomaterials* 27:2051–2059. doi:10.1021/bc0502107
- Liong M, Lu J, Kovochich M, Xia T, Ruehm SG, Nel AE, Tamanoi F, Zink JJ (2008) Multifunctional inorganic nanoparticles for imaging, targeting, and drug delivery. *ACS Nano* 2:889–896. doi:10.1021/nn800072t
- Liu X, Qiu G, Li X (2005) Shape-controlled synthesis and properties of uniform spinel cobalt oxide nanotubes. *Nanotechnology* 16:3035–3040. doi:10.1088/0957-4484/16/12/051
- Maeda H, Bharate GY, Daruwalla J (2009) Polymeric drugs for efficient tumor-targeted drug delivery based on EPR-effect. *Eur J Pharm Biopharm* 71:409–419. doi:10.1016/j.ejpb.2008.11.010
- Marin RV, Ng CH, Wilke M, Tiersch B, Fratzl P, Peter MG (2005) Size controlled hydroxyapatite nanoparticles as self-organized organic-inorganic composite materials. *Biomaterials* 26:5414–5426. doi:10.1016/j.biomaterials.2005.01.051
- Marinakos SM, Anderson MF, Ryan JA, Martin LD, Feldheim DL (2001) Encapsulation, permeability, and cellular uptake characteristics of hollow nanometer-sized conductive polymer capsules. *J Phys Chem B* 105:8872–8876. doi:10.1021/jp010820d
- Mitra S, Gaur U, Ghosh PC, Maitra AN (2001) Tumor targeted delivery of encapsulated dextran-doxorubicin conjugate using chitosan nanoparticles as carrier. *J Control Release* 74:317–323. doi:10.1016/S0168-3659(01)00342-X
- Mohapatra S, Mallick SK, Maiti TK, Ghosh SK, Pramanik P (2007) Synthesis of highly stable folic acid conjugated magnetite nanoparticles for targeting cancer cells. *Nanotechnology* 18:385102–385111. doi:10.1088/0957-4484/18/38/385102
- Panyam J, Labhasetwar V (2003) Biodegradable nanoparticles for drug and gene delivery to cells and tissue. *Adv Drug Deliv Rev* 55:329–347. doi:10.1016/S0169-409X(02)00228-4
- Papis E, Rossi F, Raspanti M, Isabella DD, Colombo G, Milzani A, Bernardini G, Gornati R (2009) Engineered cobalt oxide nanoparticles readily enter cells. *Toxicol Lett* 189:253–259. doi:10.1016/j.toxlet.2009.06.851
- Peters K, Unger RE, Gatti AM, Sabbioni E, Tsaryk R, Kirkpatrick C (2007) Metallic nanoparticles exhibit paradoxical effects on oxidative stress and proinflammatory response in endothelial cells *in vitro*. *Int J Immunopathol Pharmacol* 20:685–695
- Powder diffraction file, card 38-1420 JCPDS-ICDD International Center for Diffraction Data (1991) Swarthmore, PA

- Roa W, Xiaojing Z, Guo L, Shaw A, Hu X, Xiong Y, Gulavita S, Patel S, Sun X, Chen J, Moor R, Xing JZ (2009) Gold nanoparticles sensitize radiotherapy of prostate cancer cell by regulation of the cell cycle. *Nanotechnology* 20:1–9. doi:10.1088/0957-4484/20/37/375101
- Roco MC (2005) Environmentally responsible development of nanotechnology. *Environ Sci Technol* 39(5):94A–95A
- Sahu SK, Mallick SK, Santra S, Maiti TK, Ghosh SK, Pramanik P (2010) In vitro evaluation of folic acid modified carboxymethyl chitosan nanoparticles loaded with doxorubicin for targeted delivery. *J Mater Sci: Mater Med* 21:1587–1597. doi:10.1007/s10856-010-3998-4
- Sandhu SK, Kaur G (2002) Alterations in oxidative stress scavenger system in aging rat brain and lymphocytes. *Biogerontology* 3:161–173. doi:10.1023/A:1015643107449
- Schreiber HA, Prechl J, Jiang H, Zozulya A, Fabry Z, Denes F, Sandor M (2010) Using carbon magnetic nanoparticles to target, track, and manipulate dendritic cells. *J Immunol Methods* 356:47–59. doi:10.1016/j.jim.2010.02.009
- Sheikh FA, Barakat NAM, Kanjwal MA, Aryal S, Khil MS, Kim HY (2009) Novel self-assembled amphiphilic poly (epsilon-caprolactone)-grafted-poly (vinyl alcohol) nanoparticles: hydrophobic and hydrophilic drugs carrier nanoparticles. *J Mater Sci: Mater Med* 20:821–831. doi:10.1007/s10856-008-3637-5
- Singh R, Lillard JW Jr (2009) Nanoparticle-based targeted drug delivery. *Exp Mol Pathol* 86:215–223. doi:10.1016/j.yexmp.2008.12.004
- Steele C, Fidel PL Jr (2002) Cytokine and chemokine production by human oral and vaginal epithelial cells in response to *Candida albicans*. *Infection and Immunity* 2:577–583. doi:10.1128/IAI.70.2.577-583.2002
- Uhrich KE, Cannizzaro SM, Langer RS, Shakesheff KM (1999) Polymeric system for controlled drug release. *Chem Rev* 99:3181–3198. doi:10.1021/cr940351u
- Vauthier C, Dubernet C, Chauvierre C, Brigger I, Couvreur P (2003) Drug delivery to resistant tumors: the potential of poly (alkylcyanoacrylate) nanoparticles. *J Control Release* 93:151–160. doi:10.1016/j.jconrel.2003.08.005
- Wang K, Xu JJ, Chen HY (2005) A novel glucose biosensor based on the nanoscaled cobalt phthalocyanine-glucose oxidase biocomposite. *Biosens Bioelectron* 20:1388–1396. doi:10.1016/j.bios.2004.06.006